Analysis Of The Influence Of Divalent Substitution On The Structural, Morphological And Magnetic Properties Of Mg-Ferrites

Shuaib Mahmud,Tareq Mohammad Faruqi, Mahmudul Hasan

Abstract: This article illustrated the impact of synthesized micro-structured spinel-type polycrystalline ferrites. The technique of conventional double sintering is used $MgFe_2O_4$, $Mg_{0.5}Zn_{0.5}Fe_2O_4$, $Mg_{0.35}Cu_{0.20}Zn_{0.45}Fe_2O_4$ and $Mg_{0.35}Cu_{0.20}Zn_{0.45}Mn_{0.06}Fe_{1.94}O_4$ to investigate their impact on the size of the grain, magnetic properties and the effect of divalent substitutions. Impurity phases aren't detectable in the taken cubic spinel of single phases in the X-ray diffraction patterns. In the sample investigation it was observed that the density was tensed to increase, while the porosity decreased with the replacement of divalent ions. Microstructures show that there is an increase in grain growth as the addition of CuO is attributed to the liquid process due to CuO during sintering. At room temperature, all the samples exhibit a nice homogeneity for the sharp deterioration of μ' in μ'–T. Lower coercivity is found in all samples suggesting that the compounds are a type of soft ferrite magnets.

Index Terms: Mg- based ferrites, XRD, SEM Microstructure, Curie Temperature, Magnetic Hysteresis.

1 INTRODUCTION

THE ferrites are ceramic, polycrystalline or homogeneous materials composed of various oxides. The main element of ferrites is iron oxide. Having the closed-packed structure, spinel ferrites consists of oxygen ions followed by the formula AB_2O_4 where A refers for tetrahedral and B octahedral sites. In this noble work, variation within the composition of Mg ferrites is created to analyze the structural and magnetic characteristics. The magnetic and non-magnetic material creates an impression on their chemical, physical and mostly magnetic properties due to their divalent substitution. As a result, different characteristics of spinel ferrites have been investigating rather more interest [1-3]. Mg-based ferrites are an essential magnetic material having the useful properties of soft ferrites, high permeability, large temperature of curie, few losses, high mechanical reliability and environmental resilience[4]. The chemical composition and substitution/addition can make proper magnetic material. Tiny divalent ions can change the properties of spinel ferrites.Generally, powerfully magnetic materials such as Fe, Co, Ni, Cr, Mn etc. can change their different properties of magnetic, structural as well as in electrical in case of inclusion or delusion of nonmagnetic materials such as Li, Cu, Zn, Mg, Al etc. So the substitution of divalent ions with Mg is expected to show similar magnetic effects and regenerated structural properties in Mg ferrites. The notable impact can be seen due to some changes in factors like grain size, surface layer, sintering temperature, distributions in octahedral and tetrahedral sites [5-8]. It was well known that for high frequency application having large magnetization [9-10]. Mg-based ferrites can be used in transformer, magnetic core of coils, loudspeakers, small electric motors, gas sensors and humidity sensors due to their growing interest [11-13].

- *Shuaib Mahmud is currently working as a lecturer(corresponding author) of Electrical and Electronic Engineering at Jatiya Kabi Kazi Nazrul Islam University,Bangladesh. E-mail: shuaibmahmud@jkkniu.edu.bd*
- *Tareq Mohammad Faruqi is a lecturer of Electrical and Electronic Engineering in City University, Bangladesh. E-mail: tareq.faruqi@gmail.com*
- *Mahmudul Hasan is an assistant professor of Electrical and Electronic Engineering in Jatiya Kabi Kazi Nazrul Islam University,Bangladesh. Email: mht.apece@gmail.com*

The phase analysis with microstructural study and the observation of magnetic behavior such as curie temperature and magnetization properties are the two separated segmentation of this work.

2 METHODOLOGY OF FERRITE PREPARATION

Being usable in a different magnetic device, ferrites are prepared in either polycrystalline form or single crystal form. Several techniques were used to prepare ferrites. All of them are fallen into two categories: Conventional ceramic methodology, i.e. solid-state reaction method where milling of reactions is followed at elevated temperature by sintering technique and wet method. Sol-gel synthesis, chemical co-precipitation method, organic precursor method, reverse micelles method, co-spray roasting, activated sintering, etc. are examples of the wet method. In our research, a series of polycrystalline samples were prepared mixed of Mg ferrites. To prepare the examinee samples, the standard method of the double sintering ceramic was used. High purity oxide (99.99 percent) weighted precisely in this process. Where Fe_2O_3, CuO, MgO, ZnO, and MnO were used and this process was done focused on their molecular weight. The estimation of the weight proportion of the oxide conjugated with various samples is based on the following equation:

$$\text{Weight \% of oxide} = \frac{\text{M. wt. of oxide} \times \text{required weight of the sample}}{\text{Sum of Mol. wt. of each oxide in a sample}}$$

In this preparation process, the stoichiometric proportion was required ceramic morter and pestle and after that in the planetary ball mill, the ball was milled with different sized stainless steel balls and in ethyl alcohol media. This process had taken six (06) hours respectively to complete and the various sized stainless balls were used in this process. The disc-shaped sample which was made from the dried slurry, pre-sintered for five (05) hours at the 950°C temperature. And the sample was cooled down to room temperature at the same rate as that of heating. After crushing the sample once again to make those samples in uniformed tiny crystallites the wet ball milled in distilled water for six (06) long hours. So as to provide with chemically homogeneous and magnetically better

material this preferred lump material was crushed. Getting a homogeneous sample these oxide mixtures were milled thoroughly for 4-6 hours. Hydraulic press was used to pressurized the dried mixture which was added with Polyvinyl Alcohol to get a pellet and toroid shape respectively. Tiny amount of Saturated solution alcohol was used as a binder which was low in quantity and 1.75 ton-cm2 and 1.2 ton-cm2pressure was applied on the samples. Muffle furnace was used to sintered the samples for two (02) to three (03) hours at 1050°C-1200°C and to get rid of oxide layer the sintered samples then polished.

2.1 Ferrite preparation in Presintering method

This phase of preparing the sample is incredibly crucial because during this state of sample preparation a ferrite is made from its component oxides. The counter diffusion process is responsible for formatting the ferrites in the solid-state reaction. This means that the diffusion requires two (2) or more species of ions that initially pass across the interface of two contacting particles of different component oxides in a different direction. To form spinel ferrite, the reaction happened between Fe_2O_3 with metal oxide Mo_2o_2 during its pre-sintering stage of sample preparation. [14]:

$MO + Fe_2O_4 \longrightarrow MFe_2O_4$ (spinel)

$2\acute{M}_2O_3 + 4Fe_2O_3 \longrightarrow 4\acute{M}Fe_2O_4$ (spinel) $+O_2$

For Mg-Ferrite

$Fe_2O_3 + MgO \longrightarrow MgFe_2O_4$

For Mg-Zn Ferrite

$Fe_2O_3 + 0.5MgO + 0.5ZnO \longrightarrow Mg_{0.5}Zn_{0.5}Fe_2O_4$

For Mg-Cu-Zn Ferrite

$Fe_2O_3 + 0.35MgO + 0.20CuO + 0.45ZnO \longrightarrow Mg_{0.35}Cu_{0.20}Zn_{0.45}Fe_2O_4$

For Mg-Cu-Zn-Mn Ferrite

$Fe_{1.94}O_3 + 0.35MgO + 0.20Cu + 0.45Zn + 0.06MnO \longrightarrow Mg_{0.35}Cu_{0.20}Zn_{0.45}Mn_{0.06}Fe_{1.94}O_4$

3 Experimental Technique

3.1 X-rays study

To study the crystalline phases of the prepared samples X-ray diffractometer was used. In this diffraction technique, Cu-Kα radiation was used as a 40kV & 30mA main beam powder with nickel filter at room temperature. The sample pitch of 0.02° with a data collection rate of 1.0 second, a 2θ scan was imposed in between 20° to 70° scale to achieve possible fundamental peaks of the prepared samples where spinel phase is confirmed for all the taken samples in this XRD analysis

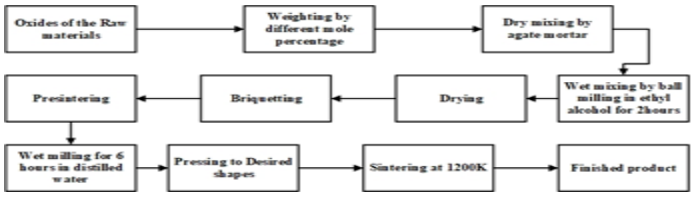

Fig. 1 Flow chart of double sintering ceramic method for ferrite material

3.2 Microstructure Determination

A scanning electron microscope ((Hitachi S 3400N, type-II, Japan) was used during this process. From the polished pellet shaped sample, we can get the micrographs. Until the micrographs are drawn, the surface of the samples will be engraved at a temperature of 1000°C below their sintering temperature for 15 minutes.

3.3 Curie Temperature Measurement

Hewlett Packard Analyzer (HP-4192A) with a small oven and a thermometer was used to measure the Curie temperature in this work. Induction method was used to calculate the temperature dependent permeability where the specimen formed the core of the coil.

3.4 Magnetization Measurement

To calculate the field dependence of magnetization the VSM 02,(Hirstlab, England) was employed at room temperature.

4 Results

4.1 XRD study

To optimize the properties of prepared samples for different applications XRD analysis is very convenient. The crystal structure identification with lattice constant determination of $MgFe_2O_4$, $Mg_{0.5}Zn_{0.5}Fe_2O_4$, $Mg_{0.35}Cu_{0.20}Zn_{0.45}Fe_2O_4$ and $Mg_{0.35}Cu_{0.20}Zn_{0.45}Mn_{0.06}Fe_{1.94}O_4$ ferrites, the total process was done by the XRD by using diffraction of X-rays (XRD). The XRD trend at room temperature of $MgFe_2O_4$, $Mg_{0.5}Zn_{0.5}Fe_2O_4$, $Mg_{0.35}Cu_{0.20}Zn_{0.45}Fe_2O_4$ and $Mg_{0.35}Cu_{0.20}Zn_{0.45}Mn_{0.06}Fe_{1.94}O_4$ ferrites were recorded by this diffraction technique where Cu-Kα radiation was used. The sample recorded a cubic spinel structure as shown in the analysis of (hkl) values of each peak (Fig. 2). It's also noticed that the peaks are all well-defined with a lack of haziness. The peaks exhibit the absence of extra peaks which defines the purity of the sample. The absence of extra peaks indicates the purity of the samples. The peaks (220), (311), (400), (422), (511) and (440) belong to the spinal period and all the peaks found correspond well to those of Mg-Zn, Mg-Cu and Mg-Cu-Zn ferrites [15-18]. The location of the peaks along with their defined miller indices is summarized in Table 1.

TABLE 1
X-ray peak positions of $MgFe_2O_4$, $Mg_{0.5}Zn_{0.5}Fe_2O_4$, $Mg_{0.35}Cu_{0.20}Zn_{0.45}Fe_2O_4$ and $Mg_{0.35}Cu_{0.20}Zn_{0.45}Mn_{0.06}Fe_{1.94}O_4$ ferrites.

Sample Ferrites	At 2θ (degree) X -ray peak positions along with miller indices					
	(220)	(311)	(400)	(422)	(511)	(440)
$MgFe_2O_4$	54.62	140.54	25.08	12.85	30.60	51.91
$Mg_{0.5}Zn_{0.5}Fe_2O_4$	81.21	227.26	40.90	24.89	60.39	72.31
$Mg_{0.35}Cu_{0.20}Zn_{0.45}Fe_2O_4$	81.95	217.55	43.55	16.51	59.94	71.86
$Mg_{0.35}Cu_{0.20}Zn_{0.45}Mn_{0.06}Fe_{1.94}O_4$	31.02	90.64	18.22	8.85	40.48	39.04

4.2 LATTICE Parameter, Bulk density, X-ray density and

POROSITY

The Nelson-Riley [19] extrapolation formula was used to get accurate values of the lattice parameter for individual samples and the data was taken from X-ray data. The Nelson-Riley formula is defined as,

$$F(\theta) = \frac{1}{2}\left[\frac{cos^2\theta}{sin\theta} + \frac{cos^2\theta}{\theta}\right]$$

where θ indicates the Bragg angle.

The relationship between the lattice parameter and the F(θ) of the sample analyzed is seen in Fig 3. All peaks are plotted to correspond to the values of 'a' denoted as lattice parameter where it was reckoned from the extrapolation straight line plotted from the Nelson-Riley function to θ values of 0 to 90 degree in F(θ) function.

The apparent density (ρ_b) of cylindrically shaped pellets was calculated using the given equation[20]

$$\rho_a = \frac{m}{V} = \frac{m}{\pi r^2 h} \quad (3)$$

Here 'r', 'm' and 'h' denotes the radius, mass, and pellet's thickness.

The ideal consistency(ρ_x) of the operative sample has been determined from the equation [20]

$$\rho_x = \frac{ZM}{Na^3} \quad (4)$$

Here Avogadro's number is N ,themolecular's weight is M and Z which is 8 for the spinel cubic structure stands for the number of the molecule per unit cell.

In this work, Porosity is also calculated from the given equation [20]

$$P = 1 - \frac{\rho_a}{\rho_x} \quad (5)$$

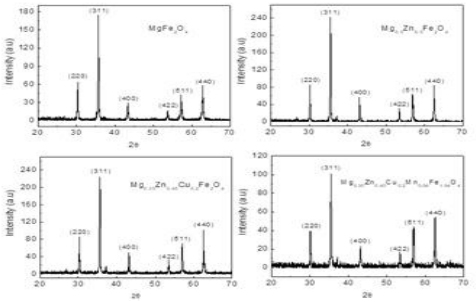

Fig. 2 *XRD Pattern of $MgFe_2O_4$, $Mg_{0.5}Zn_{0.5}Fe_2O_4$, $Mg_{0.35}Cu_{0.20}Zn_{0.45}Fe_2O_4$ and $Mg_{0.35}Cu_{0.20}Zn_{0.45}Mn_{0.06}Fe_{1.94}O_4$ ferrites.*

TABLE 2
Structural entity of samples, i.e. the lattice parameter, density and porosity

Samples	Lattice constant, a (Å)	Bulk density, ??(gm/cm^3)	X-ray density ??or ??(gm/cm^3)	Porosity P%
$MgFe_2O_4$	8.36	4.42	4.89	11.65
$Mg_{0.5}Zn_{0.5}Fe_2O_4$	8.40	4.51	4.92	8.33
$Mg_{0.35}Cu_{0.20}Zn_{0.45}Fe_2O_4$	8.41	4.65	5.01	7.18
$Mg_{0.35}Cu_{0.20}Zn_{0.45}Mn_{.06}Fe_{1.94}O_4$	8.42	4.78	5.07	5.71

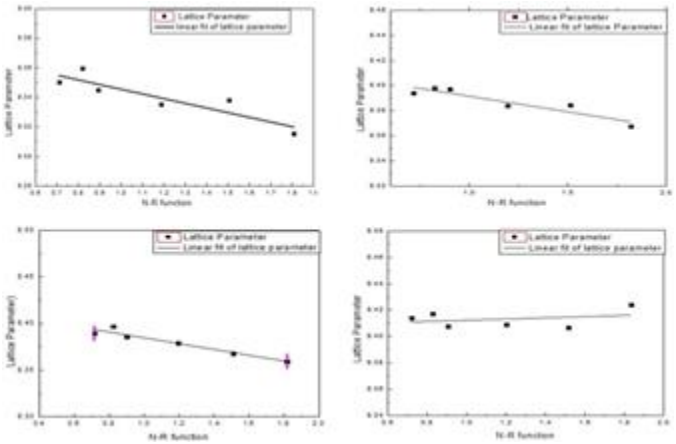

Fig. 3 Lattice parameter variance with Nelson-Riley method for all experiments

Rising in divalent levels ions(Mg^{2+}, Zn^{2+}, Cu^{2+}, Mn^{2+}) in the spinel ferrites, the ferrite lattice parameter is predicted to increase. In octahedral B-sites and tetrahedral A-sites, the physical and magnetic properties of ferrites depend to a large degree on the distribution of cations. [21]. It is well understood that the lattice constant increases proportionally with the rise of the ionic radius. The lattice parameter was stated to obey the linearity rule of Vegard's law [22] from sample-1 to sample-4. As the unit cell has increased as replaced by ions of greater ionic intensity, this improvement can be due to the ionic size difference. Although the ionic radius of Zn^{2+}(0.82Å) is greater than Mg^{2+}(0.78Å), it is predicted that the replacement will increase the lattice constant. Thus the study of fundamental properties such as Curie temperature and magnetization becomes possible with increased distance between the magnetic ions, and this distance increases with the presence of larger ions in the ferrite lattice. Values of the lattice constant of $MgFe_2O_4$ and $Mg_{0.5}Zn_{0.5}Fe_2O_4$ are 8.36Å [23] and 8.40Å. For Mg-Cu-Zn, the lattice constant increases marginally relative to Mg-Zn[24] due to incorporation of Mg^{2+}(0.78Å), Cu^{2+}(0.70Å) and Zn^{2+}(0.82Å). The lattice constant also increases for Mg-Cu-Zn-Mn[15] than Mg-Cu-Zn due to incorporation of Mg^{2+}(0.78Å), Cu^{2+}(0.70Å) [25], Zn^{2+} (0.82Å)[23] and Mn^{3+}(0.70Å)[26] dopants in the lattice.

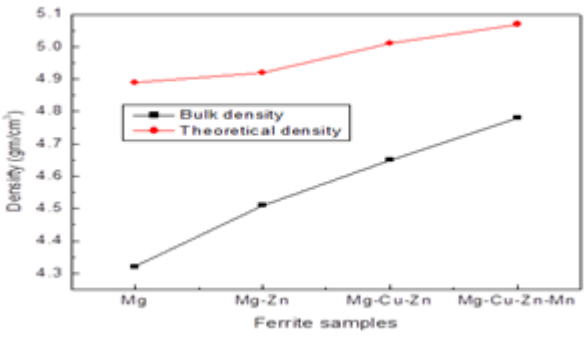

Fig. 4 *Variation of density with different ferrite samples*

The magnetic properties can also be determined by obtaining density of ferrite. By increasing the density of ferrites, elevated permeability can be achieved. The theoretical density is derived from the obtained lattice parameter, and the bulk density is calculated from the mass and volume ratio of all measured samples. A large rise in the bulk density is found in Fig.4 and Table 2 with the replacement of the material of Zn^{2+}, Cu^{2+} and Mn^{2+}.Sometimes the bulk density is observed to be less than the X-ray density. This may contribute to the presence of pores created and shaped during the sample preparation or sintering process. With the compound of Zn^{2+}, Cu^{2+} and Mn^{2+}, the porosity values of samples are greatly decreased. An indication can be found that in the densification of materials, these ions may support.

4.3 SEM MICROSTRUCTURE

In order to determine the microstructure of our prepared samples and calculate the average grain size, the scanning electron microscope was used. The samples shall be represented by the SEM microstructure in Fig.5. Basically, the microstructure depends on the sintering temperature and the substitutions used in the samples as well. The temperature allowed the pores and grain limits to be minimized during the sintering process.The reduction in pores, as a result makes the sample thick. The magnetic properties of ferrite materials have governed the grain scale. Both the sample's grain size and porosity affect the magnetic properties. If it is possible to reduce the porosity within the grain boundary[27], net magnetization can be improved. Since the grain growth rate is incredibly high, pores could also be left behind by increasingly changing grain borders, resulting in pores trapped within the grains. This intra-granular porosity, contributing to weak magnetic properties, is really difficult to remove. The sample influences the change in the size of the crop. The scale of the grain represents the existence of additional or less area for grain boundaries. Porosity may also be closely correlated with borders, since porosity can be reduced. Crop development is closely correlated with the mobility of grain boundaries. The mean grain size was obtained using the process of linear interception [28] and is shown in Table 3. As seen in Fig 5 and Table 3, the microstructure of the ferrite samples is strongly dependent on the amount of CuO present in the samples. By developing a liquid phase during sintering, the microstructure of the Mg-Zn ferrites is influenced by CuO. As a consequence of its grain boundary segregation [29], it facilitates grain growth by increasing the inter-diffusion cation density. Grain growth occurs during the sintering of the liquid phase by a dissolving/ solution-precipitation process. Tiny grains are less stable than massive grains, energetically, owing to their larger individual surface areas. As a result, within the liquid-phase layers, small grains would be dissolved. Precipitation will occur after a critical threshold is approached by the concentration of the dissolved phase. "This suggests that larger grains are growing at the expense of smaller grains. It appears that small grains need to "swim" to combine through a barrier (liquid-phase layer) with an outsized grain. It is noted that an improvement in the amount of Cu content results in an increase in the grains' liquid-phase layer coverage, and this is favorable for grain growth. Consequently, the total grain size increases as the divalent material increases.

Fig. 5(a) *SEM microstructure of* $MgFe_2O_4$ *(b) SEM microstructure of* $Mg_{0.5}Zn_{0.5}Fe_2O_4$*, (c) SEM microstructure of* $Mg_{0.35}Cu_{0.20}Zn_{0.45}Fe_2O_4$ *(d) SEM microstructure of*

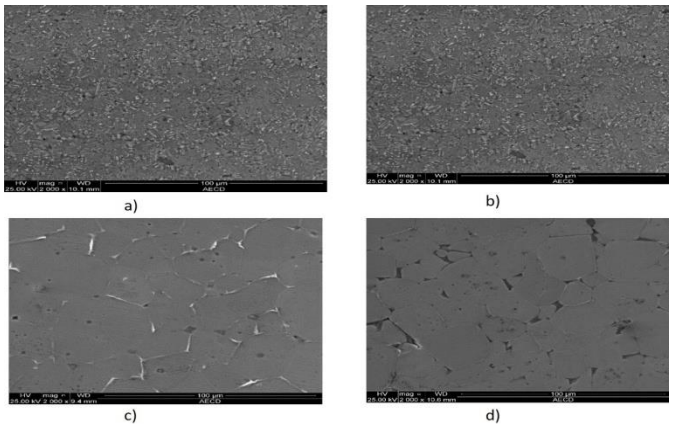

$Mg_{0.35}Cu_{0.20}Zn_{0.45}Mn_{0.06}Fe_{1.94}O_4$.

TABLE 3
Grain size of the ferrite samples.

Samples	Average grain size(μm)
$MgFe_2O_4$	07
$Mg_{0.5}Zn_{0.5}Fe_2O_4$	12
$Mg_{0.35}Cu_{0.20}Zn_{0.45}Fe_2O_4$	39
$Mg_{0.35}Cu_{0.20}Zn_{0.45}Mn_{.06}Fe_{1.94}O_4$	42

4.4 TEMPERATURE (CURIE TEMPERATURE) DEPENDENCY ON PERMEABILITY

For the toroid-shaped samples, Fig.6 demonstrates the temperature-dependence of initial permeability (μ'). It is found that the permeability increases when the temperature increases, and when the magnetic state of the ferrite samples varies from ferromagnetic to paramagnetic, it suddenly decreases above the Curie temperature, indicating that increasing thermal activation breaks the parallel alignment of the elementary magnets (spontaneous magnetisation). According to Globus [30], the sharpness of the permeability decrease at the Curie point may be used as an indicator of the degree of compositional homogeneity. As seen in Fig.6, the current ferrites display a strong degree of homogeneity. It is possible to express the difference of μ 'with temperature as follows. The constant of anisotropy (K_1) and saturation magnetization typically decreases with temperature changes. As anisotropy decreases faster than heat magnetization, the initial permeability is predicted to rise with temperature, approaches its maximum value, which is marginally below the permissible T_c and hence declines to the minimum value for the paramagnetic process. Thus the equation is based on [31].

$$\mu' \alpha \frac{{M_s}^2 D}{\sqrt{k_1}} \quad (6)$$

Where M_s is the saturation magnetization ,D is the grain diameter,μ' at the temperature at which K_1disappears, it must indicate a limit.

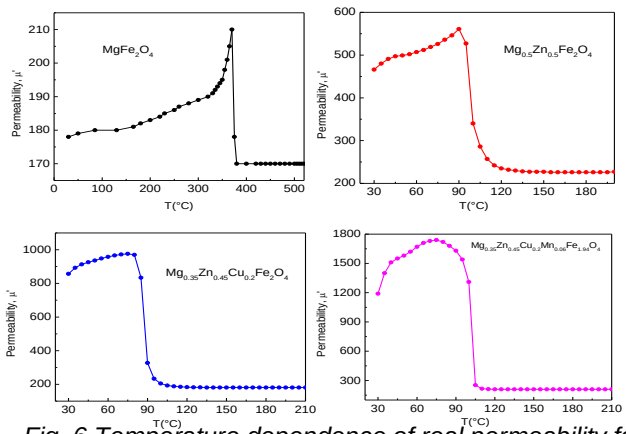

Fig. 6 Temperature dependence of real permeability for the ferrite samples

A good thermal stability of initial permeability for Mg-Zn, Mg-Cu-Zn ferrites can be seen from Fig.6, but the plateau in the μ'-T curves indicates low thermal stability of ferrites Mg and Mg-Cu-Zn-Mn. The structure of the μ'-T curve greatly depends on the composition and preparation conditions for the polycrystalline samples [32-33]. T_c is the property of the Curie temperature that is important for inductor applications and highly sensitive to composition. The ferrite curie temperature is the temperature of transformation beyond which the ferrimagnetic substance becomes paramagnetic. The temperature of the Curie gives a notion of the amount of energy needed to disrupt the long-range order within the substance. From the μ'-T curve, $T_c$of the studied ferrite system has been calculated.

TABLE 4
Data for Curie temperature (T_c) of the samples.

Samples	T_c
$MgFe_2O_4$	375
$Mg_{0.5}Zn_{0.5}Fe_2O_4$	97
$Mg_{0.35}Cu_{0.20}Zn_{0.45}Fe_2O_4$	95
$Mg_{0.35}Cu_{0.20}Zn_{0.45}Mn_{.06}Fe_{1.94}O_4$	107

The intensity of the interaction of the A-B exchange is the point on which the temperature of the Curie is primarily dependent. It is well known that the Curie temperature decreases as diamagnetic ions are added into the ferrite sub-lattice [34].The change in T_c can be related to the change in A-B exchange interaction as a result of the change in the cation distribution between A and B sub-lattices due to divalent replacement. Divalent substitution only effectively weakens the A-B interchange relationship. Due to this reduced contact of A-B exchange with divalent (Zn^{2+}, Cu^{2+}, Mn^{2+}) material, the Curie temperature is expected to decrease. By adding non-magnetic ions, the number of bonds or linkages between the magnetic ions that determine the magnitude of the Curie temperature [35] is diminished. The temperature of the curie is given in Table 4 for all the samples.

4.5 FIELD DEPENDENCE OF MAGNETIZATION BY VSM

The Vibrating Sample Magnetometer is a compact and sensitive tool invented by S to measure magnetic properties. As the sample is vibrated near it, Fonner which is centered on the flux shift in a coil. To constantly calculate the magnetic properties of the specimen as a function of field and temperature, a novel meter called the Vibrating Sample Magnetometer (VSM) is used. In this sort of magnetometer, in an area surrounded by several pick up coils, the sample is vibrated up and down. Therefore, the magnetic sample functions as a time-changing magnetic flux that varies within a selected defined area. It is to be understood from Maxwell's law that a duration differs An electric field is followed by magnetic flux, and hence the field produces a voltage in pickup coils. The alternating voltage signal is processed using a control device unit that tests the magnetization in order to extend the signal-to-noise ratio. The samples measure the room temperature magnetic hysteresis loop and the findings of the samples $MgFe_2O_4$, $Mg_{0.5}Zn_{0.5}Fe_2O_4$, $Mg_{0.35}Cu_{0.20}Zn_{0.45}Fe_2O_4$and $Mg_{0.35}Cu_{0.20}Zn_{0.45}Mn_{0.06}Fe_{1.94}O_4$ are shown in Fig.7.
No apparent hysteresis effect is seen by the hysteresis loops. Both samples had low coercivity levels, which meant that all samples belonged to the soft ferrite family.

TABLE 5
Data for Saturation Magnetization (Ms), Coercivity (Hc), Ramanent Magnetization (Mr) and Squarness(S)..

Samples	M_s(emu/gm)	H_c(oe)	M_r(emu)	S
$MgFe_2O_4$	26	28.48	0.035	0.098
$Mg_{0.5}Zn_{0.5}Fe_2O_4$	45	16.07	0.030	0.035
$Mg_{0.35}Cu_{0.20}Zn_{0.45}Fe_2O_4$	48	0.564	0.964	0.40
$Mg_{0.35}Cu_{0.20}Zn_{0.45}Mn_{0.06}Fe_{1.94}O_4$	54	15.23	0.016	0.018

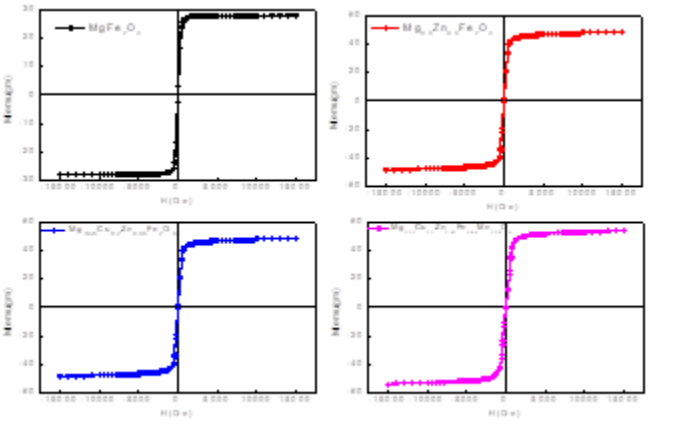

Fig. 7 Hysteresis curves of the samples $MgFe_2O_4$, $Mg_{0.5}Zn_{0.5}Fe_2O_4$, $Mg_{0.35}Cu_{0.20}Zn_{0.45}Fe_2O_4$and $Mg_{0.35}Cu_{0.20}Zn_{0.45}Mn_{0.06}Fe_{1.94}O_4$ ferrites.

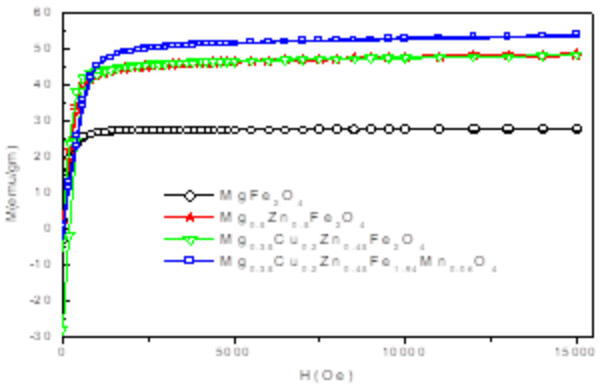

Fig. 8 *Magnetization curves of the samples* $MgFe_20_4$, $Mg_{0.5}Zn_{0.5}Fe_2O_4$, $Mg_{0.35}Cu_{0.20}Zn_{0.45}Fe_2O_4$*and* $Mg_{0.35}Cu_{0.20}Zn_{0.45}Mn_{0.06}Fe_{1.94}O_4$ *ferrites.*

The magnetization curves (M-H) of room temperatures are shown in Fig.8 as a function of the field. For the samples at room temperature, saturation magnetization Ms as shown in Table 5. It is observed that with increasing divalent content, saturation magnetization improves (Mg-Zn, Mg-Cu-Zn, Mg-Cu-Zn-Mn). In terms of the different exchange interactions, such as A-B, A-A, and B-B, the observed disparity in saturation magnetization, which depends on the distribution of magnetic and non-magnetic ions at the A and B sites, may be explained. It is understood that the A-B interaction is the strongest and that the B-B and A-A interactions are dominant. In this multi-cationic complex system, the difference in saturation magnetization with various divalent concentrations can be due to the re-arrangement of the cation distribution between the A and B sub-lattices. The stable ions of Zn^{2+} indicate a preference for the spinel lattice tetrahedral (A-sites)[36] and Fe^{3+}ions in the Mg-Zn ferrite partly occupy A-sites and B-sites[37]. On Mg^{2+}ions, most B-sites are located and a small fraction migrates to A-sites[38]. Saturation magnetization is given by M_s= M_B - M_A according to Neel's model of ferrimagnetism for two sub-lattice[39], where M_B represents the octahedral and M_A represents tetrahedral sub-lattice magnetization. The improvement in the value of M is due to the fact that Cu^{2+} ions ideally appear to go to the B-sites by replacing Mg^{2+}ions and just a slight increase in the B-sites' magnetic moment in order to increase the net magnetic moment.A maximum value of 54 emu/gm of Mg-Cu-Zn-Mn ferrite is obtained by saturation magnetization.

5 Conclusion

The variation in composition in X-ray diffraction confirms the spinel structure of the ferrite samples which exhibits signified improvement in bulk density of Mg-ferrites. And there is a improved grain growth and grain size. In this work, the sharp fall of µ'was found in samples that reflect the strong homogeneity of the samples. The introduction of Zn^{2+}, Cu^{2+} and Mn^{2+} ions causes a decrement in Curie temperature. The increment in divalent content causes the slightest increment in saturation magnetization of samples.

Acknowledgment

The authors are thankful to the Material Science Division (MSD) of the Atomic Energy Center (AECD), Dhaka-1000, Bangladesh, for enabling sample preparation for the use of laboratory facilities with full-scale generous cooperation.

References

[1] Y.I. Kim, D. Kim, C.S. Lee, Synthesis and characterization of CoFe2O4 magnetic nanoparticles prepared by temperature-controlled coprecipitation method, Physica B 337 (2003) 42–51.

[2] C. Caizer, M. Popovici, C. Savii, Spherical (ZnδNi1−δFe2O4)γ nanoparticles in an amorphous (SiO2)1−γ matrix, prepared with the sol–gel method, Acta Mater. 51 (2003) 3607–3616

[3] D.K. Kim, Y. Zhang, W. Voit, K.V. Rao, M. Muhammed, Synthesis and characterization of surfactant-coated superparamagnetic monodispersed iron oxide nanoparticles, J. Magn. Magn. Mater. 225 (2001) 30–36

[4] RumanaZahir (2010) "Study of the Structural, Magnetic and Electrical Properties of Magnesium-Cadmium Ferrites" Department of Physics, Chittagong University of Engineering and Technology, Chittagong, Bangladesh

[5] Tan M, K¨ oseo˘glu Y, Alan F and S¸ ent ¨ urk E 2011 J. Alloys Compd. 5099399

[6] Patange S, Shirsath S E, JangamLohar G K, Jadhav S S and Jadhav K 2011 J. Appl. Phys. 109 053909

[7] Islam M U, Abbas T, Niazi S B, Ahmad Z, Sabeen S and Chaudhry M A 2004 Solid State Commun. 130 353

[8] He X M, Yan S M, Li ZW, Zhang X, Song X Y, QiaoW, ZhongW and Du Y W 2015 Chin. Phys. B 24 127502

[9] T. Nakamura, "Snoek's Limit in High-Frequency Permeability of Polycrystalline Ni-Zn, Mg-Zn, and Ni- Zn-Cu Spinel Ferrites," Journal of Applied Physics, Vol. 88, No. 1, 2004, pp. 348-353 Surname A and Surname B 2009 Journal Name23 544

[10] P.B. Belavi, G.N. Chavan, L.R. Naik, R. Somashekar, R.K. Kotnala. "Structural, electrical and magnetic properties of cadmium substituted nickel–copper ferrites"; Materials Chemistry and Physics Volume 132, Issue 1, 16 January 2012, Pages 138-144

[11] Q. Chen and Z. J. Zhang, Appl. Phys. Lett. 71, 3156 (1998).

[12] F. A. Benko and E. P. Koffyberg, Mater. Res. Bull. 21, 1183 (1986).

[13] Z. Tinashu, P. Hing, Z. Jianeheng, and K. Kingbing, Mater. Chem. Phys. 61, 192 (1999).

[14] P. Reijnen, Reactivity of Solids, Fifth International Symposium (Edited by G.-M. Schwab), p. 562. Elsevier, Amsterdam (1965); (c) C. Kooy, ibid. p. 21. (d) G. C. Kuczynskii, Ferrites, Proc. Int. Conf., 1970 (Edited by Y. Hoskino, S. Lida and M. Sugimoto), p, 87. Univ. Tokyo Press, Japan (1971).

[15] M. M. Haque, M. Huq and M. A. Hakim, "Thermal Hysteresis of Permeability and Transport Properties of Mn Substituted Mg-Cu-Zn Ferrites," Journal of Physics D: Applied Physics, Vol. 41, No. 5, 2008, 10 p

[16] M. M. Haque, M. Huq and M. A. Hakim, "Influence of CuO and Sintering Temperature on the Microstructure and Magnetic Properties of Mg-Cu-Zn Ferrites," Journal of Magnetism and Magnetic Materials, Vol. 320, No. 21, 2008, pp. 2792-2799

[17] N. Reslescu, E. Reslescu, C. L. Sava, F. Tudorache and P.D. Popa, "On the Effects of Ga3+ and La3+ Ions in MgCu Ferrite: Humidity-Sensitive Electrical Conduction," Crystal Research Technology, Vol. 39, No. 6, 2004, pp. 548-557

[18] A. Bhaskar, B. R. Kanth and S. R. Murthy, "Electrical Properties of Mn Added MgCuZn Ferrites Prepared by Microwave Sintering Method," Journal of Magnetism and Magnetic Materials, Vol. 283, No. 1, 2004, pp. 109-116

[19] J. B. Nelson and D. P. Riley, “An Experimental Investigation of Extrapolation Methods in the Derivation of Accurate Unit-Cell Dimensions of Crystals,” Proceedings of the Physical Society (London), Vol. 57, No. 3, 1945, p.160
[20] M. Aliuzzaman, M. Manjurul Haque, M. JannatulFerdous, S. ManjuraHoque, M. Abdul Hakim, “ Effect of Sintering Time on the Structural, Magnetic and Electrical Transport Properties of Mg0.35Cu0.20Zn0.45Fe1.94O4 Ferrites” , World Journal of Condensed Matter Physics, 2014, 4, 13-23
[21] G. P. Kumar, V. Raghavendra and C. P. Babu, Chem. Sci. Trans. 5 (2016) 1096
[22] L. Vegard, Phys. 5 (1921) 17.
[23] Alex Goldman,” Handbook of Modern Ferromagnetic Materials’,Kluwer Academic publisher, Norwell, Masschusettapagw, page-210,(1999)
[24] H.Z.Wang and L.G.Dong,Proc.2nd Int. Symp.Phys.Mang.Mat; p-211,(1992)
[25] S.M. Yunus, H.S.Shim, C.H.Lee, M.A.Asgar, F.U.Ahmed, A.K.M Zakaria, “Neutron diffraction studies of the diluted spinel ferrite ZnxMg0.75−xCu0.25 Fe2O4” , Journal of Magnetism and Magnetic Materials Volume 232, Issue 3, July 2001, Pages 121-132
[26] B.P.Ladgaonkar,P,N.Vasambaker,A.S.Vaingankar,J.Magn,Magn. Mater.210(2000).
[27] P.B. Belavi, G.N. Chavan, L.R. Naik, R. Somashekar, R.K. Kotnala. “Structural, electrical and magnetic properties of cadmium substituted nickel–copper ferrites”; Materials Chemistry and Physics Volume 132, Issue 1, 16 January 2012, Pages 138-144.
[28] M. I. Mendelson, J. Am. Ceram. Soc. 52(8) (1969) 443.
[29] K. O. Low, F. R. Sale, J. Magn. Magn. Mater. 246 (2002) 30
[30] A. Globus, H. Pascard and V. Cagan, J. Phys. Coll. 38 (1977) C1–C163
[31] G. C. Jain, B. K. Das, R. S. Khanduja and S. C. Gupta, “ Effect of intragranular porosity of initial permeability and coercive force in a manganese zinc ferrite”, Journal of Materials Science, July 1976, Volume 11, Issue 7, pp 1335–1338
[32] E. Reslescu, L. Sachelarie and N. Reslescu, “Influence of copper ions on the structure and electromagnetic properties of MgZnferrite ” , JOURNAL OF OPTOELECTRONICS AND ADVANCED MATERIALS Vol. 8, No. 3, June 2006, p. 1019 – 1022
[33] Z.-X. Yue, J. Zhou, L.-T. Li, X.-H. Wang and Z.-L. Gui, “Effect of copper on the electromagnetic properties of Mg–Zn–Cu ferrites prepared by sol–gel auto-combustion method” Materials Science and Engineering: Volume 86, Issue 1, 4 September 2001, Pages 64-69
[34] J. Smit and H. P. J. Wijn, “Ferrites (Philips Tech. Library (Netherlands),” 1959
[35] R. Mitra, R. K. Pure and R. G. Mendiratta, “Magnetic and electrical properties of hot-pressed Ni-Zn-Li ferrites” Journal of Materials Science, March 1992, Volume 27, Issue 5, pp 1275–1279.
[36] Z.-X. Yue, J. Zhou, L.-T. Li, X.-H. Wang and Z.-L. Gui, Mater. Sci. Eng. B 86 (2001) 64
[37] R. Jotania, R. Upadhay and R. Kulkarni, “Magnetic ordering in Zn substituted Co/sub 1.4/Ge/sub 0.4/Fe/sub 1.2/O/sub 4/ spinel system” IEEE Transactions on Magnetics (Volume: 28 , Issue: 4 , July 1992), Page(s): 1889 – 1894
[38] R. Kulkarni and H. Joshi, Solid State Commun. 53 (1985) 1005.
[39] L. Neel, Ann. De Phys. 3 (1948) 137